DOI: 10.1002/chem.200700496

Self-Assembly of Nanosize Coordination Cages on Si(100) Surfaces

Marco Busi,[a] Marco Laurenti,[a] Guglielmo G. Condorelli,[b] Alessandro Motta,[b] Maria Favazza,[b] Ignazio L. Fragalà,[b] Marco Montalti,[c] Luca Prodi,[c] and Enrico Dalcanale*[a]

Dedicated to Professor David N. Reinhoudt on the occasion of his 65th birthday

Abstract: Bottom-up fabrication of 3D organic nanostructures on Si(100) surfaces has been achieved by a two-step procedure. Tetradentate cavitand **1** was grafted on the Si surface together with 1-octene (Oct) as a spatial spectator by photochemical hydrosilylation. Ligand exchange between grafted cavitand **1** and self-assembled homocage **2**, derived from cavitand **5** bearing a fluorescence marker, led to the formation of coordination cages on Si(100). Formation, quantification, and distribution of the nanoscale molecular containers on a silicon surface was assessed by using three complementary analytical techniques (AFM, XPS, and fluorescence) and validated by control experiments on cavitand-free silicon surfaces. Interestingly, the fluorescence of pyrene at $\approx$4 nm above the Si(100) surface can be clearly observed.

Keywords: coordination cages · fluorescence · self-assembly · silicon surfaces · surface analysis

Introduction

Self-assembly is the most promising approach to build organic nanostructures on surfaces, leading to hybrid organic–inorganic materials.[1] The idea behind this approach is to exploit the thermodynamic control and reversibility of self-assembly for the error-free generation of 3D architectures directly on surfaces, which is one of the key requirements for the development of nanotechnology[2] and molecular electronics.[3] So far, most of the activity has been concentrated on gold surfaces, due to the easy access to SAMs (self-assembled monolayers)[4] as substrates for further derivatizations.[5,6] As most of the devices are Si-based, the ability to generate 3D nanoscopic structures on silicon represents an important step forward in the direction of Si-integrated hybrid organic–inorganic materials. Surface hydrosilylation of H-terminated silicon wafers has emerged as a promising strategy for grafting organic molecules onto inorganic surfaces[7] for the development of molecular devices able to perform specific functions. The two major obstacles hindering the development of Si-based hybrid materials are: 1) the lack of self-assembly protocols of 3D objects operating on Si surfaces and 2) the precise characterization of these hybrid materials, which can only be approached by using several complementary techniques. As a first step in this direction, we report the coordination cage self-assembly (CSA) on Si and the thorough characterization of the resulting surfaces by using a combination of XPS (X-ray photoelectron spectroscopy), AFM (atomic force microscopy), and fluorescence spectroscopy. Coordination cages are appealing molecular containers[8] because of their peculiar properties, comprising stabilization of reactive intermediates,[9] catalysis,[10] and reversibility, which allows guest uptake and release under controlled conditions.[11] For cavitand-based coordination cages the transfer of the self-assembly protocol from solution[12] to gold surfaces has already been worked out.[13]

[a] Dr. M. Busi, M. Laurenti, Prof. E. Dalcanale
Dipartimento di Chimica Organica ed Industriale University of Parma
and INSTM UdR Parma V.le G. P. Usberti 17 A
43100 Parma (Italy)
Fax: (+39) 0521-905472
E-mail: enrico.dalcanale@unipr.it

[b] Prof. G. G. Condorelli, A. Motta, M. Favazza, Prof. I. L. Fragalà
Dipartimento di Scienze Chimiche University of Catania
and INSTM UdR Catania V.le A. Doria 6
95100 Catania (Italy)

[c] Dr. M. Montalti, Prof. L. Prodi
Dipartimento di Chimica "G. Ciamician"
Latemar Unit University of Bologna Via Selmi 2
40126, Bologna (Italy)

Supporting information for this article is available on the WWW under http://www.chemeurj.org/ or from the author.

Results and Discussion

The Si-surface functionalization required a two-step procedure (Scheme 1): 1) grafting the cavitand **1**/1-octene (Oct) mixture on a Si–H surface by photochemical hydrosilylation[7] and 2) CSA of cages **3** by ligand exchange on this surface by using a solution of preformed homocage **2**. The "capping" cavitand forming the grafted heterocage **3** has been designed to add a powerful and sensitive technique, namely fluorescence spectroscopy, to AFM and XPS to prove the effectiveness of the self-assembly on silicon protocol. A pyrene derivative was chosen as a fluorescent unit because of its high emission efficiency and its ability to give both monomeric and excimeric emission bands and, as a consequence, to signal the presence of other pyrenes to its closeness on surfaces.[14] The functionalization with only one pyrene molecule for each cavitand was carried out to avoid the formation of intramolecular excimers so that the eventual presence of an excimer band in the fluorescence emission could be attributed to intermolecular interactions.

Synthesis of grafting cavitand 1: This cavitand is a tetradentate ligand, presenting four tolylpyridine derivatives at the upper rim for metal coordination and four terminal double bonds at the lower rim for grafting on silicon wafers. The presence of four outwardly oriented rigid groups is pivotal for the self-assembly of the coordination cage. The synthesis of cavitand **1** is outlined in Scheme 2. The reaction of resorcinarene **4** with 4–4′-(α,α-dibromo)tolylpyridine led to the exclusive formation of the outward (*oooo*) isomer in 25% yield.

Cavitand 1 grafting on a Si(100) surface: The cavitand grafting procedure was performed by means of photochemical hydrosilylation on a H-terminated Si(100) surface. The etching procedure of the bare silicon wafer and the photochemical reaction variables were optimized according to a previous work.[15] The use of Oct as a spatial spectator in the mixed monolayers with cavitand **1** satisfies two requirements. The first was to reach an optimal coverage of the Si surface, thus minimizing the oxidation of the substrate after the grafting[17] and the second was to dilute the cavitand presence on the surface to avoid interdigitation of the tolylpyridine groups in nearby cavitands, which jeopardizes CSA.[13] A 1:4 molar ratio between cavitand **1** and Oct turned out to be the maximum cavitand concentration allowed in the starting grafting solution to fulfill the two requirements.

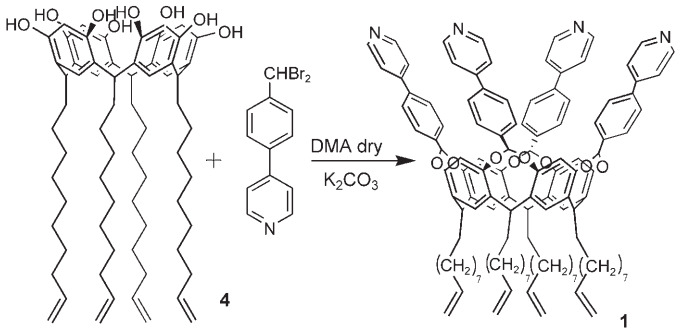

Scheme 2. Synthesis of cavitand **1** used for the grafting on silicon wafers.

Synthesis of capping cavitand 5: Cavitand **5** is also a tetradentate ligand, presenting four outwardly oriented tolylpyridine groups for the self-assembly and a single fluorophore unit appended at the lower rim. The synthesis consists of two steps (Scheme 3), the bridging of the resorcinarene **6** phenolic OHs with 4–4′-(α,α-dibromo)tolylpyridine, followed by the esterification of the terminal alcohol at the lower rim of the cavitand **7** with 1-carboxypyrene acid.

Self-assembly of the homocage 2: Self-assembly of the homocage **2** in solution was performed to see if the fluorescence emission of the pyrene unit is retained after CSA. The self-assembly procedure consisted of the addition of two [Pt(dppp)(OTf)$_2$] complex equivalents to a cavitand **5** solution dissolved in [D$_2$]dichloromethane (Scheme 4). Fluo-

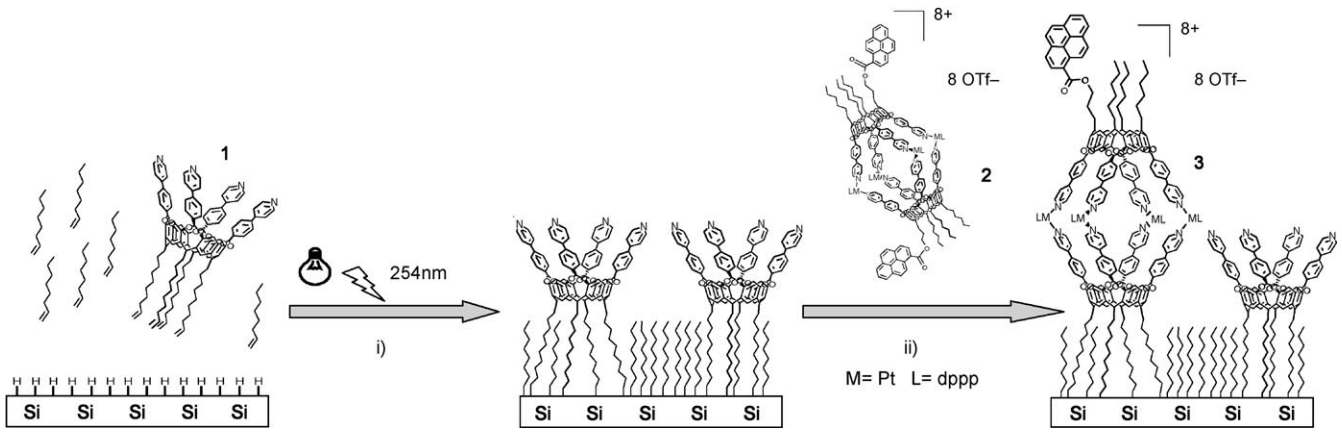

Scheme 1. i) Grafting on the etched Si surface of a cavitand **1**/Oct mixed monolayer from a mesitylene solution of the organic compounds, ii) CSA of cage **3** on a Si surface by ligand exchange with homocage **2** dissolved in a CH_2Cl_2 solution.

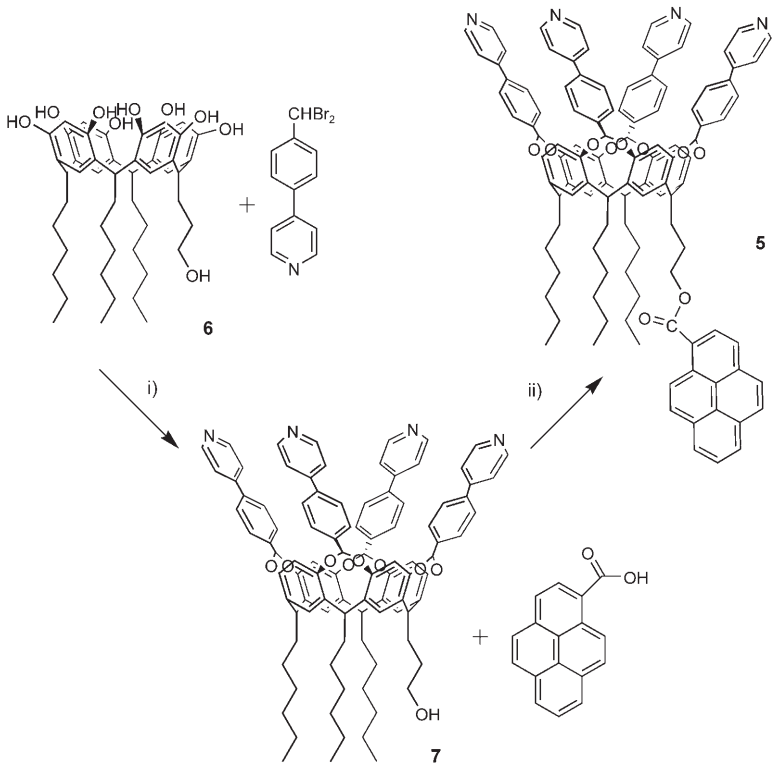

Scheme 3. Synthetic pathway to fluorescent cavitand **5**. i) DMA dry, K_2CO_3, 80 °C, 16 h, ii) CH_2Cl_2, DMAP, DCC, RT, 3 d.

rescence spectra of cavitand **5** and homocage **2** (Figure 4a) in aerated dichloromethane showed a typical monomeric band of pyrene with a very high fluorescence quantum yield ($\Phi = 0.43$ for **5** and $\Phi = 0.44$ for **2**) and an excited-state lifetime τ of 4.9 (5) and 4.8 ns (2), indicating that the formation of the four Pt complexes has no influence on the photophysical properties of the pyrene chromophore.

Self-assembly of the heterocage 3 on a silicon surface: The silicon substrate with a cavitand **1**/Oct mixture-grafted monolayer was dipped into a solution of homocage **2**, formed by the addition of cavitand **5** and [Pt(dppp)(OTf)$_2$], in dichloromethane ($2.2 \cdot 10^{-4}$ M). The formation of the grafted heterocage **3** requires ligand exchange between homocage **2** in solution and grafted cavitand **1** (Scheme 1). Ligand exchange between cages, already verified in solution,[16] led to the smooth and clean formation of heterocage **3** directly on the surface. After 3 h at 25 °C, the substrate was taken out of solution, and rinsed thoroughly with ethanol and dichloromethane to eliminate any physisorbed species on the surface. As a control experiment, the same procedure was performed also on a pure Oct-grafted silicon substrate. Surface XPS and AFM characterizations were performed after each step.

XPS: The elemental compositions of the alternate prepared samples are summarized in Table 1. XPS analyses of the grafted cavitand **1**/Oct layer showed the presence of all expected elements. The observation of the N 1s band, mainly centered at 399.9 eV, is diagnostic of cavitand **1** grafting. The experimental N/C atomic ratio is consistent with the atomic N/C ratio calculated for the molar composition of the initial cavitand **1**/Oct grafting solution. After CSA, XPS analysis showed the presence of new elements, namely Pt, F, and S (Table 1 and Figure S2 in the Supporting Information). The formation of cage **3** is supported by the presence of a signal in the Pt 4f region. In particular, the 4f 7/2 component centered at 73.0 eV is diagnostic of a Pt^{II} species (Figure 1a).[17] In order to verify that the presence of the Pt signal was associated to cage **3** formation, a pure Oct-grafted substrate underwent the same treatment. In this case, no signal was detected in the Pt region (Figure 1b). In addition, the F/Pt and S/Pt ratios are about 6 and 2, as expected for octacationic cage **3** surrounded by eight OTf^- counterions. Note that the N/Pt atomic ratio (28) is much higher than the value (2) expected for a self-assembling process occurring on an all-grafted cavitand **1**, thus indicating that CSA on the surface occurs in low yield (about 4%, see the Experimental Section for calculation).[18] No angular dependence of the Pt signals has been observed, ruling out attenuation effects due to the presence of the capping cavitand **5**. This is reasonable, assuming that the coordination cages are isolated. Partial success of the capping reaction is not surprising considering the dilute conditions employed and that not all cavitands on the Si surface are grafted in the correct orientation for CSA. Moreover, partial self-assembly is useful for a proper section analysis of the silicon surface by AFM (see the next section), by evidencing the height differences between the two species (cavitands and cages) on the same substrate.

AFM: AFM characterizations were performed in a high-amplitude mode (tapping mode) to avoid any possible modification of the grafted organic layer on the surfaces caused by the interactions with the tip. First, to support the experimental AFM data, Spartan[19] MMFF force-field calculations of single cavitand **1** and grafted heterocage **3** with respect to the Oct-grafted layer were performed with the purpose of evaluating the dimensions of the objects. The lowest-energy conformer of each structure is shown in Figure 2a,b. All the substrate characterizations were performed after cleaning

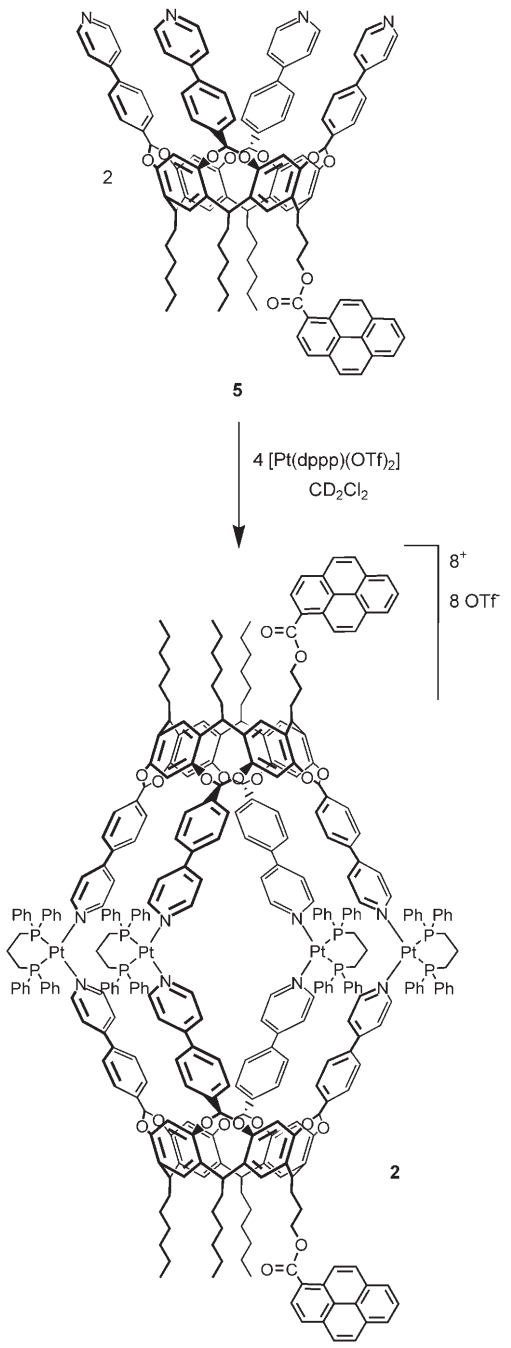

Scheme 4. Self-assembly of fluorescent homocage **2**.

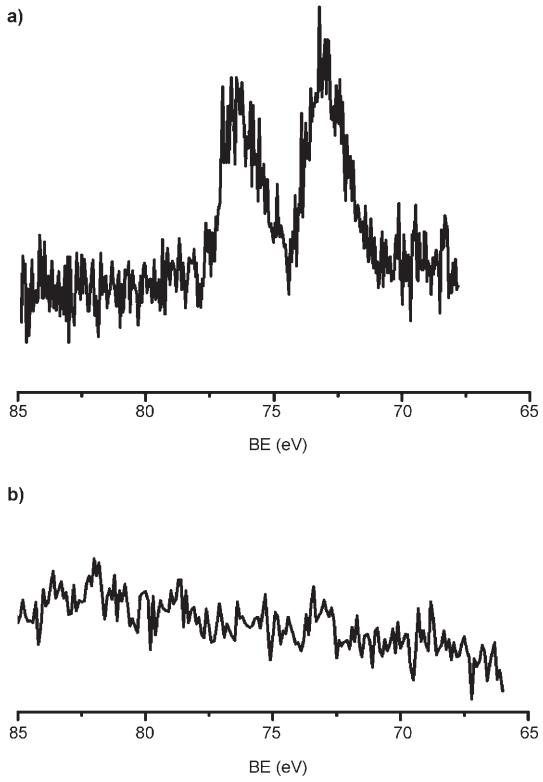

Figure 1. High resolution Pt 4f XPS spectra of Si substrates after the CSA on a) 20% cavitand **1**-grafted monolayer and b) pure Oct-grafted monolayer.

procedures, which consisted of rinsing with ethanol and dichloromethane, followed by drying with a nitrogen flux. At least four topographies of 4 μm^2 areas in different positions were recorded for all surfaces (Figure 3). For the 20% cavitand **1** grafted silicon surface (Figure 3a) several topographies on different areas showed the presence of reproducible peaks that protrude from the Oct-grafted layer. The height of those peaks is compatible with the dimension calculated in Figure 2a. After the CSA protocol and the rinsing procedure, reproducible peaks with a height compatible with the dimensions of the heterocage **3** (Figure 2b) appeared on the substrate (Figure 3b, peaks A, B, and C), in addition to the cavitands already found before the self-assembly (peaks D and E). No peaks ascribable to cavitands or cages were found on the pure Oct-grafted Si substrate exposed to the same CSA treatments (Figure 3c). The AFM topographies of the control experiment with the pure Oct-grafted layer shows both the effectiveness of the rinsing procedure after the CSA protocol aimed to remove all the physisorbed species on the substrate and the impossibility to generate any kind of supramolecular structure on a cavitand-free surface. Region analyses on the 4 μm^2 topographies of Figure 3 showed the absence of peaks protruding from the surface more than 4 nm for wafers a) and c) (Figures S3–S5 in the Supporting Information), while in the case of wafer b), the percentage of peaks above

Table 1. Elemental composition of a) cavitand **1**/Oct 1:4 decorated silicon surface, b) cavitand **1**/Oct decorated surface after CSA and c) control sample constituted of Oct decorated surface after CSA (take-off angle 45°).

	Atomic fractions [%][a]							Atomic ratios		
	Si	O	C	N	Pt	F	S	N/C	F/Pt	N/Pt
a)	39.4	16.0	42.1	1.1	–	–	–	0.026	–	–
b)	23.4	32.1	42.7	1.4	0.05	0.32	≈0.08	0.033	6.4	28
c)	36.3	31.5	31.8	≈0.2	–	–	–			

[a] The presence of P cannot be determined as the P 2s peak is hidden by the more intense plasmon loss band of Si

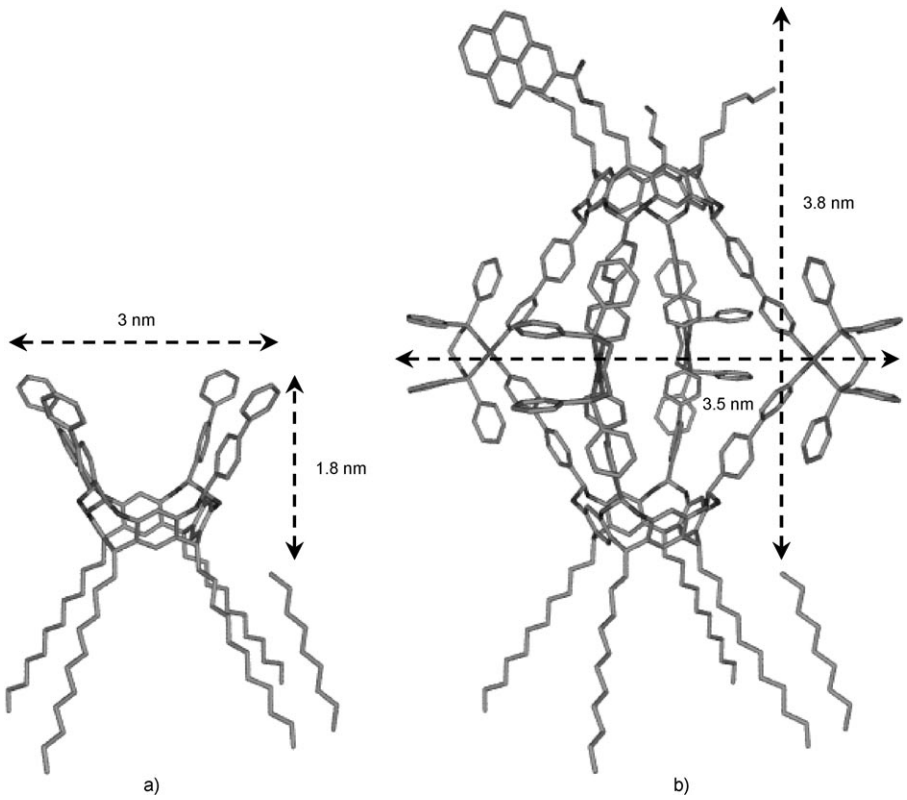

Figure 2. Molecular modeling and dimensions of the grafted cavitand **1** a) and the heterocage **3** b) with respect to grafted Oct.

this value (grafted heterocage **3**, Figure 2b) is about 4.5%. This value is close to the 4% estimate obtained by XPS analysis. The fact that two independent and complementary techniques converge toward similar values validates the estimate of a 4% cage formation on silicon under the reported conditions.[18]

Fluorescence emission: Fluorescence measurement in reflectance on the silicon substrates before and after the self-assembles were carried out. The relatively efficient emission of the pyrene excimeric form with respect to the monomeric one is useful to indicate the distribution of the pyrene molecules present on the surface. In order to visualize a low number of fluorophore molecules on the surface, a powerful source, namely a He–Cd laser with a 325 nm emission was used. To check the reproducibility of the fluorescence emission spectra recorded, many measurements at different surface areas were performed for the analyzed substrates. The resulting spectra are shown in Figure 4. Fluorescence spectra of physisorbed homocages **2**, obtained by solvent evaporation of the solution used for the surface CSA on a pure Oct-grafted substrate showed both the presence of the structured monomer band and of a strong excimer pyrene band (Figure 4d), while pure Oct-grafted substrates, exposed to CSA and rinsing procedures, did not show any fluorescence emission (Figure 4b) for all the investigated areas. The cage **3** decorated Si surface showed instead (Figure 4c) a structured fluorescence band, similar to the one typical of the pyrene monomer, although slightly red-shifted. The red shift of the fluorescence band of pyrene with respect to the measurement in solution represented in Figure 4a can be attributed to long-range electronic perturbations associated with the electric field of the silicon surfaces, as observed for the same chromophore when bound to gold nanoparticles.[14a,20] To our knowledge, this is the first example of the observation of fluorescence of a dye covalently linked on a Si(100) surface. The absence of the excimeric band in Figure 4c indicates that the anchored heterocages **3** are isolated and not clustered on the surface, in agreement with AFM measurements.

Conclusion

A new route to Si-integrated hybrid organic–inorganic materials has been demonstrated through the self-assembly of 3D nanosize coordination cages on Si(100) surfaces. The formation of these 3D supramolecular structures on surfaces by a self-assembly protocol is fully demonstrated by three independent analytical techniques (AFM, XPS, and fluorescence) and verified by the absence of self-assembled cages on a cavitand-free-grafted silicon surface as a control experiment. This methodology offers the advantages of an easy, high fidelity access to complex 3D structures associated with the possibility of introducing specific probes to test the presence and distribution of the obtained species on silicon. In the specific case examined, pyrene turned out to be an efficient probe, as its fluorescence can still be observed at $\approx$4 nm from the Si(100) surface. As no clustering of the supramolecular structures was observed, this methodology is amenable to be employed with a single-molecule addressing of encapsulated guests. Work is in progress to adapt the self-assembly procedure towards the inclusion of large guests, such as single-molecule magnets.[21]

Experimental Section

General: All commercial reagents were ACS reagent grade and used as received. For the syntheses, all solvents were dried over 3 and 4 Å molecular sieves. For the surface procedures, all the solvents used were HPLC grade microfiltrated on 0.45 μm pore membranes, the glassware was

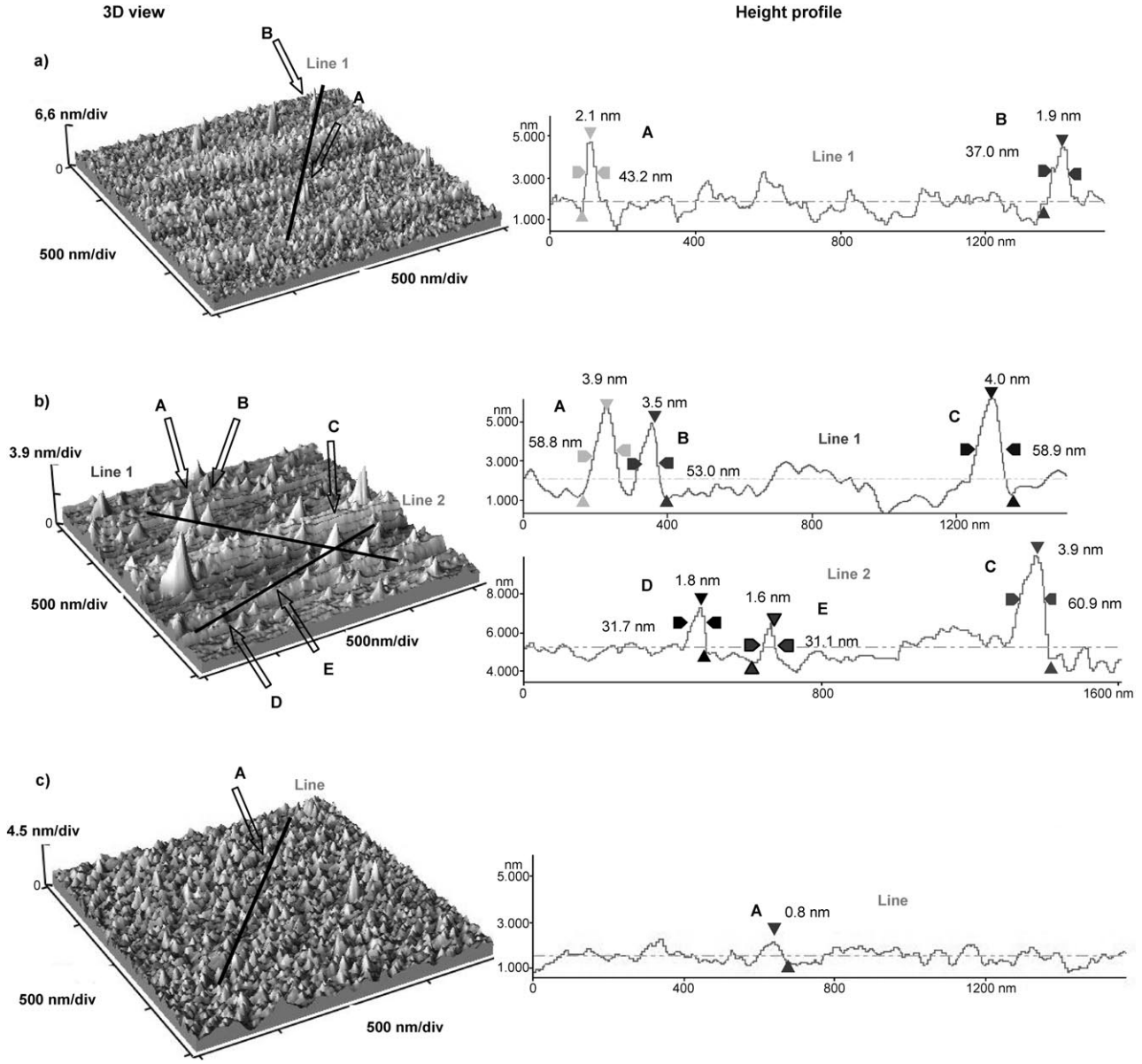

Figure 3. TM-AFM images, 3D view and cross-section analysis of a) mixed cavitand **1**/Oct-grafted monolayer, b) heterocage **3**/cavitand **1**-grafted substrate after CSA and rinsing procedure, c) pure Oct-grafted substrate after CSA and rinsing procedure.

treated with piranha solution (concentrated H_2SO_4/H_2O_2 2:1 v/v) and washed with bidistillate water Millipore grade. ^1H NMR spectra were recorded on Bruker AVANCE (300 MHz) spectrometers and all chemical shifts (δ) were reported in parts per million (ppm) relative to the proton resonances resulting from incomplete deuteration of the NMR solvents. ESIMS experiments were performed on a Waters ZMD spectrometer equipped with an electrospray interface. MALDI-TOF MS spectra were obtained on a PerSpective Biosystems Voyager DE-RP spectrometer equipped with delayed extraction. Column chromatography was performed by using silica gel 60 (Merck 70–230 mesh). Absorption spectra in solution were recorded on a Perkin–Elmer Lambda 40 spectrophotometer. Fluorescence spectra in solution were obtained with a 450 W Xe lamp and excited-state lifetimes in solutions were obtained with a modular UV/visible NIR spectrofluorimeter, Edinbourg, equipped with a single-photon counting apparatus. Corrections for instrumental response, inner filter effects and phototube sensitivity were performed.[22] Quinine sulfate in H_2SO_4 0.5 M ($\Phi = 0.55$) was used as a standard for fluorescence quantum yields.[22] Fluorescence spectroscopy on Si surfaces were obtained with a spectrofluorimeter ISA FLUOROLOG 3 by using a He–Cd continuum laser at 325 nm with a 50 mW power. Atomic force microscopy (AFM) characterization was performed on a Thermomicroscopes (VEECO) Autoprobe CP research instrument, equipped with a 5 μm high-resolution scanner in high amplitude mode (tapping mode). The used tips were the NSG 11 model of the NT-MDT. Computational analyses of the substrates topography were performed with Image Processing and Data Analyses v. 2.1.15 software. X-ray photoelectron spectroscopy (XPS) spectra of the substrates were run with a PHI 5600 ESCA/SAM multitechnique spectrometer equipped with a Mg standard and a monochromated Al Kα X-ray source. The analyses were carried out at a 10–45° photoelectron angle (relative to the sample surface) with an acceptance angle of ±7°. XPS B.E. scale was calibrated by centering the C 1s peak due to hydrocarbon moieties at 285.0 eV.[23,24]

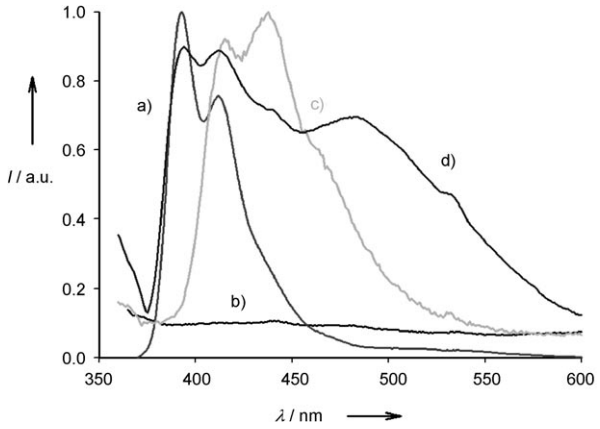

Figure 4. Emission fluorescence spectra ($\lambda_{exc}=325$ nm) of: a) Aerated dichloromethane solution of homocage **2**, b) pure Oct-grafted on the silicon substrate after CSA, c) Self-assembled heterocages **3** on the Si substrate surface, d) thin layer of physisorbed fluorescent homocages **2** deposited on an Oct-grafted substrate.

Resorcinarene **4**,[25] resorcinarene **6**,[26] 4–4′-(α,α-dibromo)tolylpyridine,[13] and [Pt(dppp)(OTf)$_2$] [27] (dppp = 1,3-bis(diphenylphosphino)propane and OTf$^-$ = $CF_3SO_3^-$) were prepared according to literature procedures.

Cavitand 1: 4,4′-(α,α-Dibromo)tolylpyridine (4.00 g, 12.2 mmol) and K_2CO_3 (4.04 g , 29.0 mmol) were added, under nitrogen, to a solution of resorcinarene **4** (2.54 g, 2.44 mmol) in dry DMA (DMA = dimethylacetimide; 30 mL). The mixture was stirred in a sealed tube at 80 °C for 16 h. The reaction was quenched by the addition of water and the resulting mixture was extracted with CH_2Cl_2. The organic layer was washed with water (3 × 15 mL), dried on Na_2SO_4, and evaporated. The crude product was purified by column chromatography on silica gel by using CH_2Cl_2/ethanol (9:1 v/v) as eluant to give compound **1** as pale-yellow solid (1.02 g, 0.60 mmol, 25 %). ^{1}H NMR (300 MHz, $CDCl_3$, 23 °C, TMS): δ = 8.68 (d, ^3J = 5.3 Hz, 8H), 7.83 (d, ^3J = 8.4 Hz, 8H), 7.72 (d, ^3J = 8.4 Hz, 8H), 7.51 (d, ^3J = 5.9 Hz, 8H), 7.31 (s, 4H), 6.74 (s, 4H), 5.87–5.77 (m, 4H), 5.56 (s, 4H), 5.03–4.92 (m, 12H), 2.37–2.34 (m, 8H), 2.07–2.04 (m, 8H), 1.50–1.25 ppm (m, 48H); MS (MALDI-TOF): *m*/*z* (%): calcd for $C_{116}H_{124}N_4O_8$: 1701.9 $[M+H]^+$; found: 1701.8 (100).

Cavitand 7: 4,4′-(α,α-Dibromo)tolylpyridine (2.34 g, 7.15 mmol) and K_2CO_3 (2.59 g, 18.7 mmol) were added, under nitrogen, to a solution of resorcinarene **6** (1.10 g, 1.37 mmol) in dry DMA (30 mL). The mixture was stirred in a sealed tube at 80 °C for 16 h. The reaction was quenched by the addition of water and the resulting mixture was extracted with CH_2Cl_2. The organic layer was washed with water (3 × 15 mL), dried on Na_2SO_4, and evaporated. The crude product was purified by column chromatography on silica gel by using CH_2Cl_2/ethanol (9:1 v/v) as eluant to give compound **7** as pale-yellow solid (0.34 g, 0.23 mmol, 17 %). ^{1}H NMR (300 MHz, $CDCl_3$, 23 °C, TMS): δ = 8.67 (d, ^3J = 5.1 Hz, 8H), 7.83 (d, ^3J = 8.1 Hz, 8H), 7.72 (d, ^3J = 8.4 Hz, 8H), 7.52 (d, ^3J = 6.0 Hz, 8H), 7.36 (s, 2H), 7.30 (s, 2H), 6.74 (s, 4H), 5.57 (s, 4H), 4.98 (t, ^3J = 8.4 Hz, 4H), 3.85 (t, ^3J = 6.0 Hz, 2H), 2.54–2.48 (m, 2H), 2.41–2.31 (m, 6H), 1.76–1.71 (m, 2H,), 1.48–1.26 (m, 18H), 0.93 ppm (m, 9H); MS (MALDI-TOF): *m*/*z* (%): calcd for $C_{97}H_{94}N_4O_9$: 1459.7 $[M+H]^+$; found: 1459.4 (100).

Cavitand 5: 1-Pyrenecarboxilic acid (0.025 g, 0.103 mmol), DCC (DCC = 1,3-dicyclohexylcarbodiimide; 0.021 g, 0.103 mmol), and DMAP (DMAP = 4-dimethylaminopyridine; 0.012 g, 0.103 mmol) were stirred at 0 °C for 30 minutes in 15 mL of dry CH_2Cl_2 and three drops of dry DMA. The mixture was stirred at room temperature for 30 min under argon and cavitand **7** (0.1 g, $6.85\cdot10^{-2}$ mmol) were added. The mixture was stirred at room temperature for 3 d. The reaction was quenched by the addition of water, and the resulting mixture was extracted with CH_2Cl_2. The organic layer was evaporated and dried to give a pale-yellow solid. This solid was then sonicated in methanol, filtered, and dried. The crude product was purified by column chromatography on silica gel by using CH_2Cl_2/ethanol (9:1 v/v) as eluant to give compound **5** as pale-yellow solid (0.069 g, $4.85\cdot10^{-2}$ mmol, 17 %). ^{1}H NMR (300 MHz, $CDCl_3$, 23 °C, TMS): δ = 9.33 (d, ^3J = 9.6 Hz, 1H), 8.66 (br d, 8H), 8.26–8.05 (m, 8H), 7.81 (d, ^3J = 6.9 Hz, 8H), 7.73 (d, ^3J = 5.7 Hz, 8H), 7.52 (d, ^3J = 5.7 Hz, 8H), 7.38 (s, 2H), 7.33 (s, 2H), 6.74 (s, 4H), 5.56 (s, 4H), 5.18 (t, ^3J = 8.1 Hz, 1H), 4.99 (t, ^3J = 8.1 Hz, 3H), 4.70 (t, ^3J = 6.3 Hz, 2H), 2.66 (m, 2H), 2.36 (m, 6H), 1.42–1.23 (m, 20H), 0.89 ppm (m, 9H); MS (ESI): *m*/*z* (%): calculated for $C_{114}H_{104}N_4O_{10}$: 1689.8 $[M+H]^+$; found: 1688.8 (100).

Self-assembly of homocage 2 in solution: The cage formation was monitored by ^{1}H NMR spectroscopy whilst gradually adding [Pt(dppp)(OTf)$_2$] (1.55 mg, $1.7\cdot10^{-3}$ mmol) dissolved in CD_2Cl_2 to a solution of cavitand **5** (1.45 mg, $8.6\cdot10^{-4}$ mmol). ^{1}H NMR (300 MHz, CD_2Cl_2, 23 °C, TMS): δ = 9.23 (br d, 2H), 9.01 (br d, 8H), 8.63 (br d, 2H), 8.31–8.01 (m, 16H), 7.77–7.12 (m, 136H), 6.68 (s, 8H), 5.05 (m, 2H), 4.86 (m, 4H), 4.63 (m, 2H), 3.33 (m, 16H), 2.93 (m, 8H), 2.63 (m, 4H), 2.33 (m, 12H), 1.62 (m, 52H), 0.90–0.81 ppm (m, 18H); ^{31}P NMR (162 MHz, CD_2Cl_2, 23 °C, H_3PO_4): δ = −15.02 ppm (t, ^2J(Pt,P) = 3136 Hz; 8P); MS (ESI): *m*/*z* (%): calcd for $C_{344}H_{304}O_{44}N_8Pt_4P_8S_8F_{24}$: 6998.8 $[M]+$, 3350.3 $[M-2\,OTf]^{2+}$, 2183.9 $[M-3\,OTf]^{3+}$, 1600.6 $[M-4\,OTf]^{4+}$; found: 3348.7 (80), 2183.5 (60), 1600.3 (30).

Monolayer preparation: Cavitand **1**/1-octene mixtures with 0.2 cavitand mole fraction were dissolved in mesitylene (solution concn = 0.05 M) for grafting of the monolayer. Cavitand solution (2 mL) was placed in a quartz cell and was deoxygenated by stirring in a dry box for at least 1 h. Subsequently, a Si(100) substrate was etched in 2.5 % hydrofluoric acid for 2 min, quickly rinsed in water, and immediately placed in the solution. The cell remained under UV irradiation (254 nm) for 2 h. The sample was then removed from the solution and sonicated in CH_2Cl_2 for 10 min.

Preparation of the cavitand 1 and pure 1-octene-grafted silicon substrates for AFM analyses: All the cavitands grafted and pure Oct–Si wafers were cleaned with an ultrasound bath in dichloromethane for 2 min, then rinsed with ethanol, dichloromethane, and dried with a nitrogen flux before AFM characterization.

Self-assembly of coordination heterocages 3 on silicon substrates: The Si wafers with 20 % grafted cavitands **1** were soaked in a 2.2×10^{-4} M solution of homocages **2** obtained by mixing cavitand **5** (3.7 mg, 2.19 mmol) and [Pt(dppp)(OTf)$_2$] complex (4.5 mg, 4.94 mmol) in CH_2Cl_2 (5 mL) for 3 h at 25 °C. Removed from the solution, the substrates were rinsed with ethanol, dichloromethane, and dried with a nitrogen flux. As a control experiment, the substrate with only pure Oct grafted underwent the same self-assembly and rinsing protocol (Figure 4d). The same solution of self-assembled homocages **2** was used for the deposition of a thin layer (50 μL, $1.1\cdot10^{-5}$ mmol) of physisorbed cages by solvent evaporation on Oct-grafted substrate for the fluorescence characterization.

Assessment of the CSA on silicon: The yield of cage formation is given by the percentage of the reacted cavitand **1** (% cav **1**) on the Si surface:

$$\%\,\text{cav}\,\mathbf{1} = \frac{\text{reacted cav}\,\mathbf{5}\,\text{molecules}}{\text{total cav}\,\mathbf{1}\,\text{molecules}} \times 100 = \frac{\%N_{\text{cav}\mathbf{5}}}{\%N_{\text{cav}\mathbf{1}}} \times 100 \quad (1)$$

The atomic percentage of nitrogen (%N) on the surface after CSA is due to nitrogen atoms of the total cavitand **1** ($\%N_{cav\mathbf{1}}$) and reacted cavitand **5** ($\%N_{cav\mathbf{5}}$) in self-assembled cages:

$$\%N = \%N_{cav\mathbf{1}} + \%N_{cav\mathbf{5}} \quad (2)$$

As self-assembly of cavitand **5** requires a Pt atom for each cavitand nitrogen, the value for $\%N_{cav\mathbf{5}}$ must be equal to the observed atomic percentage of Pt. Therefore, $\%N_{cav\mathbf{1}} = \%N - \%Pt$ can be derived from Equation (2) and Equation (1) can be rewritten as follows:

$$\%\,\text{cav}\,\mathbf{1} = \frac{\%Pt}{\%N - \%Pt} \times 100 \quad (3)$$

From Equation (3) and the data in Table 1, the amount of self-assembled cavitand **1** can be deduced as about 4 %. The estimated error is about 1 %, deriving from a set of six different measurements.

Acknowledgements

This work was supported by MUR through COFIN 2005 (Strategie molecolari e supramolecolari per la deposizione di magneti a singola molecola orientati su superfici), FIRB 2003–2004 LATEMAR and by the EU through NoE MAGMANet (3-NMP 515767–2). We thank Professor L. Cristofolini (University of Parma) for help with the AFM instrumentation. The instrumental facilities at the Centro Interfacoltà di Misure G. Casnati of the University of Parma were used. We thank one of the referees for useful suggestions regarding the AFM data treatment.

[1] a) A. B. Descalzo, R. Martinez-Manez, F. Sancenon, K. Hoffmann, K. Rurack, *Angew. Chem.* **2006**, *118*, 6068–6093; *Angew. Chem. Int. Ed.* **2006**, *45*, 5924–5948; b) J. M. Buriak, *Chem. Rev.* **2002**, *102*, 1271–1308.

[2] a) R. F. Service, *Science* **2000**, *290*, 1524–1531; b) R. F. Service, *Science* **2005**, *309*, 95.

[3] C. Joachim, J. K. Gimzewski, A. Aviram, *Nature* **2000**, *408*, 541–548.

[4] J. C. Love, L. A. Estroff, J. K. Kriebel, R. Nuzzo, G. M. Withesides, *Chem. Rev.* **2005**, *105*, 1103–1169.

[5] T. P. Sullivan, W. T. S. Huck, *Eur. J. Org. Chem.* **2003**, *1*, 17–29.

[6] S. Onclin, J. Huskens, B. J. Ravoo, D. N. Reinhoudt, *Small* **2005**, *1*, 852–857.

[7] a) M. R. Linford, P. Fenter, P. M. Eisenberg, C. E. D. Chidsey, *J. Am. Chem. Soc.* **1995**, *117*, 3145–3155; b) A. B. Sieval, A. L. Demirel, J. M. Nissink, J. H. van der Maas, W. H. De Jeu, H. Zuilhof, E. J. R. Sudhölter, *Langmuir* **1998**, *14*, 1759–1768; c) Q.-Y. Sun, L: C. P. M. d Smet, B. van Lagen, M. Giesberg, P. C. Thune, J. Van Engelenburg, F. A. d Wolf, H. Zuilhof, E. J. R. Sudhölter, *J. Am. Chem. Soc.* **2005**, *127*, 2514–2523.

[8] D. J. Cram, J. M. Cram, Container Molecules and Their Guests (Ed.: J. F. Stoddart), Royal Society of Chemistry, **1994**.

[9] a) M. Yoshizawa, Y. Takeyama, T. Okano, M. Fujita, *J. Am. Chem. Soc.* **2000**, *122*, 6311–6312; b) M. Yoshizawa, K. Kumazawa, M. Fujita, *J. Am. Chem. Soc.* **2005**, *127*, 13456–13457.

[10] a) H. Ito, T. Kusukawa, M. Fujita, *Chem. Lett.* **2000**, *29*, 598–599; b) M. Yoshizawa, M. Tamura, M. Fujita, *Science* **2006**, *312*, 251–254; c) D. H. Leung, R. G. Bergman, K. N. Raymond, *J. Am. Chem. Soc.* **2006**, *128*, 9781–9797.

[11] a) P. Jacopozzi, E. Dalcanale, *Angew. Chem.* **1997**, *109*, 665–667; *Angew. Chem. Int. Ed. Engl.* **1997**, *36*, 613–615; b) O. D. Fox, N. K. Dalley, R. G. Harrison, *J. Am. Chem. Soc.* **1998**, *120*, 7111–7112.

[12] R. Pinalli, V. Cristini, V. Sottili, S. Geremia, M. Campagnolo, A. Caneschi, E. Dalcanale, *J. Am. Chem. Soc.* **2004**, *126*, 6516–6517.

[13] E. Menozzi, R. Pinalli, E. A. Speets, B. J. Ravoo, E. Dalcanale, D. N. Reinhoudt, *Chem. Eur. J.* **2004**, *10*, 2199–2206.

[14] a) M. Montalti, L. Prodi, N. Zaccheroni, G. Battistini, *Langmuir* **2004**, *20*, 7884–7886; b) M. Montalti, L. Prodi, N. Zaccheroni, M. Beltrame, T. Morotti, S. Quici, *New J. Chem.* **2007**, *31*, 102–108.

[15] G. G. Condorelli, A. Motta, M. Favazza, I. L. Fragalà, M. Busi, E. Menozzi, E. Dalcanale, L. Cristofolini, *Langmuir* **2006**, *22*, 11126–11133.

[16] L. Pirondini, F. Bertolini, B. Cantadori, F. Ugozzoli, C. Massera, and E. Dalcanale, *Proc. Natl. Acad. Sci. USA* **2002**, *99*, 4911–4915.

[17] a) G. M. Bancroft, T. Chan, R. J. Puddenphatt, M. P. Brown, *Inorg. Chim. Acta* **1981**, *53*, L119 L120; b) W. M. Riggs, *Anal. Chem.* **1972**, *44*, 830–832; c) P. Brant, J. H. Enemark, A. L. Balch, *J. Organomet. Chem.* **1976**, *114*, 99–106.

[18] No attempts have been made to maximize the yield of coordination cages on the Si surface.

[19] Spartan 04, Wavefunction, Inc., http://www.wavefun.com.

[20] P. Anger, P. Bharadway and L. Novotny, *Phys. Rev. Lett.* **2006**, *96*, 113002.

[21] A. L. Barra, A. Caneschi, A. Cornia, F. Fabrizi De Biani, D. Gatteschi, C. Sangregorio, R. Sessoli, L. Sorace, *J. Am. Chem. Soc.* **1999**, *121*, 5302–5310.

[22] M. Montalti, A. Credi, L. Prodi, M. T. Gandolfi, *Handbook of Photochemistry*, 3rd ed., CRC Taylor & Francis, Boca Raton **2006**.

[23] P. Swift, *Surf. Interface Anal.* **1982**, *4*, 47–51.

[24] G. F. Cerofolini, C. Galati, S. Lorenti, L. Renna, O. Viscuso, C. Bongiorno, V. Raineri, C. Spinella, G. G. Condorelli, I. L. Fragalà, A. Terrasi, *Appl. Phys. A* **2003**, *77*, 403–409.

[25] U. E. Thoden van Velzen, J. F. J. Engbersen, D. N. Reinhoudt, *Synthesis* **1995**, 989–997.

[26] F. Hauke, A. J. Myles, J. Rebek Jr, *Chem. Commun.* **2005**, *33*, 4164–4166.

[27] P. J. Stang, D. H. Cao, S. Saito, A. M. Arif, *J. Am. Chem. Soc.* **1995**, *117*, 6273–6283.

Received: March 29, 2007
Published online: May 30, 2007

